



Fermi National Accelerator Laboratory

FERMILAB-Pub-93/332-E

E687

Precise Measurements of the D^0 and D^+ Meson Lifetimes

**P.L. Frabetti et al
The E687 Collaboration**

*Fermi National Accelerator Laboratory
P.O. Box 500, Batavia, Illinois 60510*

November 1993

Submitted to *Physics Letters B*



Disclaimer

This report was prepared as an account of work sponsored by an agency of the United States Government. Neither the United States Government nor any agency thereof, nor any of their employees, makes any warranty, express or implied, or assumes any legal liability or responsibility for the accuracy, completeness, or usefulness of any information, apparatus, product, or process disclosed, or represents that its use would not infringe privately owned rights. Reference herein to any specific commercial product, process, or service by trade name, trademark, manufacturer, or otherwise, does not necessarily constitute or imply its endorsement, recommendation, or favoring by the United States Government or any agency thereof. The views and opinions of authors expressed herein do not necessarily state or reflect those of the United States Government or any agency thereof.

Precise Measurements of the D^0 and D^+ Meson Lifetimes

P. L. Frabetti⁽¹⁾ H. W. K. Cheung⁽²⁾ J. P. Cumalat⁽²⁾ C. Dallapiccola^{a(2)} J. F. Ginkel⁽²⁾
S. V. Greene⁽²⁾ W. E. Johns⁽²⁾ M. S. Nehring⁽²⁾ J. N. Butler⁽³⁾ S. Cihangir⁽³⁾ I. Gaines⁽³⁾
P. H. Garbincius⁽³⁾ L. Garren⁽³⁾ S. A. Gourlay⁽³⁾ D. J. Harding⁽³⁾ P. Kasper⁽³⁾
A. Kreymer⁽³⁾ P. Lebrun⁽³⁾ S. Shukla⁽³⁾ M. Vittone⁽⁶⁾ S. Bianco⁽⁴⁾ F. L. Fabbri⁽⁴⁾
S. Sarwar⁽⁴⁾ A. Zallo⁽⁴⁾ R. Culbertson⁽⁵⁾ R. W. Gardner⁽⁵⁾ R. Greene⁽⁵⁾ J. Wiss⁽⁵⁾
G. Alimonti⁽⁶⁾ G. Bellini⁽⁶⁾ B. Caccianiga⁽⁶⁾ L. Cinquini^{c(6)} M. Di Corato⁽⁶⁾
M. Giammarchi⁽⁶⁾ P. Inzani⁽⁶⁾ F. Leveraro⁽⁶⁾ S. Malvezzi^{d(6)} D. Menasce⁽⁶⁾ E. Meroni⁽⁶⁾
L. Moroni⁽⁶⁾ D. Pedrini⁽⁶⁾ L. Perasso⁽⁶⁾ A. Sala⁽⁶⁾ S. Sala⁽⁶⁾ D. Torretta^{b(6)} D. Buchholz⁽⁷⁾
D. Claes^{e(7)} B. Gobbi⁽⁷⁾ B. O'Reilly⁽⁷⁾ J. M. Bishop⁽⁶⁾ N. M. Cason⁽⁸⁾ C. J. Kennedy^{f(8)}
G. N. Kim⁽⁸⁾ T. F. Lin⁽⁸⁾ D. L. Pušeljčić⁽⁸⁾ R. C. Ruchti⁽⁸⁾ W. D. Shephard⁽⁸⁾
J. A. Swiatek⁽⁸⁾ Z. Y. Wu⁽⁸⁾ V. Arena⁽⁹⁾ G. Boca⁽⁹⁾ C. Castoldi⁽⁹⁾ G. Gianini⁽⁹⁾
S. P. Ratti⁽⁹⁾ C. Riccardi⁽⁹⁾ P. Vitulo⁽⁹⁾ A. Lopez⁽¹⁰⁾ G. P. Grim⁽¹¹⁾ V. S. Paolone⁽¹¹⁾
P. M. Yager⁽¹¹⁾ J. R. Wilson⁽¹²⁾ P. D. Sheldon⁽¹³⁾ F. Davenport⁽¹⁴⁾ J. F. Filaseta⁽¹⁵⁾
G. R. Blackett⁽¹⁶⁾ M. Pisharody⁽¹⁶⁾ T. Handler⁽¹⁶⁾ B. G. Cheon⁽¹⁷⁾ J. S. Kang⁽¹⁷⁾
K. Y. Kim⁽¹⁷⁾

(E687 Collaboration)

(1) *Dip. di Fisica dell'Università and INFN - Bologna, I-40126 Bologna, Italy.*

(2) *University of Colorado, Boulder, CO 80309.*

(3) *Fermilab, Batavia, IL 60510.*

(4) *Laboratori Nazionali di Frascati dell'INFN, I-00044 Frascati, Italy.*

(5) *University of Illinois at Urbana-Champaign, Urbana, IL 61801.*

(6) *Dip. di Fisica dell'Università and INFN - Milano, I-20133 Milano, Italy.*

(7) *Northwestern University, Evanston, IL 60208.*

(8) *University of Notre Dame, Notre Dame, IN 46556.*

(9) *Dip. di Fisica Nucleare e Teorica dell'Università and INFN - Pavia, I-27100 Pavia, Italy.*

(10) *University of Puerto Rico at Mayaguez, Puerto Rico.*

(11) *University of California-Davis, Davis, CA 95616.*

(12) *University of South Carolina, Columbia, SC 29208.*

(13) *Vanderbilt University, Nashville, TN 37235.*

(14) *University of North Carolina-Asheville, Asheville, NC 28804.*

(15) *Northern Kentucky University, Highland Heights, KY 41076.*

(16) *University of Tennessee, Knoxville, TN 37996.*

(17) *Korea University, Seoul 136-701, Korea.*

(November 8, 1993)

Abstract

We report precise measurements of the D^0 and D^+ meson lifetimes by the E687 Collaboration at Fermilab. The measurements have been made using 16,000 fully reconstructed decays of the D^0 into the $K^-\pi^+$ and $K^-\pi^+\pi^-\pi^+$ final states and 9,000 decays of the D^+ into the $K^-\pi^+\pi^+$ final state. The lifetimes of the D^0 and D^+ mesons are measured to be $0.413 \pm 0.004 \pm 0.003$ ps and $1.048 \pm 0.015 \pm 0.011$ ps respectively.

This paper reports new precise measurements of the D^0 and D^+ meson lifetimes from data collected in high energy photoproduction experiment E687 during the 1990/91 Fermilab fixed target physics run.

The E687 detector, a large aperture multiparticle magnetic spectrometer with excellent vertex measurement, particle identification, and calorimetric capabilities, is described in detail elsewhere [1]. It utilized a high energy bremsstrahlung photon beam with average tagged photon momentum of 220 GeV/c and a beryllium target.

To obtain clean charm samples in $K^-\pi^+$, $K^-\pi^+\pi^-\pi^+$ and $K^-\pi^+\pi^+$ decays, all daughter candidates were required to have acceptable tracks in both microstrip and multiwire proportional tracking systems with consistent track parameters, and be appropriately identified by the Čerenkov system. The distinct topology of charm events (i.e., the existence of two spatially separated vertices) provides the single most powerful tool to isolate the signal from the non-charm background. Therefore, the value of the spatial separation ℓ between the reconstructed production and decay vertices divided by its error σ_ℓ was used as a detachment cut variable. The standard E687 “candidate-driven” vertexing algorithm [1] was used to form the secondary (decay) vertex from candidate tracks and then seed the primary (production) vertex with the reconstructed charm vector. The confidence levels for the hypotheses that the selected tracks form secondary and primary vertices were required to be greater than 1%. In addition, the fiducial region for decays was defined to end at the first trigger counter (TR1) in order to avoid the region of partial detection and reconstruction efficiency for charmed particles decaying very close to or within the microstrip system.

High energy photon-beryllium interactions produce $J=0$ (D^0, D^+) as well as $J=1$ (D^{*0}, D^{*+}) charm mesons among other products. (States and their charge conjugates are implied in this paper except where otherwise explicitly stated.) Thus a fraction of the observed D^0 's come from the decay chain $D^{*+} \rightarrow \pi^+ D^0$. It is thus natural to partition the total sample into “no-tag” and “tag” events according to their origin. Events are placed in the “tag” sample if a pion of the correct charge can be combined with the reconstructed D^0 such that the invariant mass difference $M(\pi^+ D^0) - M(D^0)$ lies within ± 2 MeV/c² of

the accepted [2] $D^{*+} - D^0$ mass difference. The pion candidates were selected from among all the tracks reconstructed in the multiwire proportional system not already belonging to the charm vertex. Candidates that fail the tagging criteria form the “no-tag” sample statistically independent from the former. In addition to the requirements listed above, events with primary vertices formed only by the reconstructed charm vector and a single track were removed in order to reduce possible systematic bias from incorrectly identified primary vertices. Figures 1 and 2 show the invariant mass distributions for the four D^0 and one D^+ sample for particular choice of l/σ_l detachment cut. The charm signal yields, presented with the figures, are deduced from fits to the mass distributions with a Gaussian peak over a linear background.

The lifetimes were measured using a binned maximum likelihood fitting technique [3]. A fit was made to the reduced proper time distribution of the events in the signal region. The reduced proper time is given by $t' = (l - N\sigma_l)/\beta\gamma c$, where N represents the significance of detachment cut used, and $\beta\gamma$ is the laboratory frame Lorentz boost of the charm meson. The signal region reduced proper time distribution was formed from events with invariant mass within $\pm 2\sigma_m$ of the mean D mass (± 0.028 GeV/ c^2 for $K^-\pi^+$, ± 0.020 GeV/ c^2 for $K^-\pi^+\pi^-\pi^+$, and ± 0.022 GeV/ c^2 for $K^-\pi^+\pi^+$). The binned maximum likelihood method allows direct use of the proper time distribution of the data above and below the D mass peak to represent the background underneath the signal instead of using a background parameterization. We have chosen two sidebands starting $4\sigma_m$ above and below the mean D mass, each half as wide as the signal region. The signal and background reduced proper time distributions were binned in proper time resolution wide bins (0.05ps) spanning six nominal lifetimes.

The observed numbers of events in a reduced proper time bin i (centered at t'_i) in the signal and side band histograms are labeled s_i and b_i respectively. The predicted number of events n_i in a reduced proper time bin is given by

$$n_i = (N_s - B) \frac{f(t'_i) \exp(-t'_i/\tau)}{\sum f(t'_i) \exp(-t'_i/\tau)} + B \frac{b_i}{\sum b_i},$$

where N_s is the total number of events in the signal region, B is the total number of background events in the signal region and $f(t'_i)$ is a correction factor. The fit parameters are B and τ . The $f(t')$ correction factor, derived from Monte Carlo simulation, corrects the reduced proper time evolution of the signal for the effects of geometric acceptance, analysis cuts, hadronic absorption, and decay of charm secondaries. Fig. 3 and Fig. 4c) display $f(t')$ as a function of t' for the four D^0 and the D^+ sample respectively. The $f(t')$ factors do not vary significantly with t' over the whole reduced proper time interval with the exception of the $K^-\pi^+\pi^+$ case. The fall off in $f(t')$ for the D^+ case is due to exclusion of long lived events with vertices downstream of the TR1 cut.

A factor \mathcal{L}_{bg} is included in the likelihood function in order to relate B to the number of background events expected from the side band population. The background level is thereby jointly determined from the invariant mass distribution and from the reduced proper time evolution in the side bands. The likelihood function is then given by

$$\mathcal{L} = \mathcal{L}_{signal} \times \mathcal{L}_{bg}$$

where

$$\mathcal{L}_{signal} = \prod_{i=1}^{bins} \frac{n_i^{s_i}}{s_i!} \exp(-n_i)$$

and

$$\mathcal{L}_{bg} = \frac{(\mu_{bg})^{N_{bg}}}{N_{bg}!} \exp(-\mu_{bg})$$

with $N_{bg} = \sum b_i$ and $\mu_{bg} = B/R$ where R is the ratio of widths of the signal and side band mass regions.

The fitted lifetime is plotted versus the ℓ/σ_{ℓ} detachment cut used for the four D^0 samples in Fig. 5 and the single D^+ sample in Fig. 4a). The five displayed lifetimes show no significant variation with the ℓ/σ_{ℓ} cut employed. The value of the ℓ/σ_{ℓ} detachment cut at which to quote the lifetime was chosen by minimizing the systematic uncertainty of the measurement while preserving its statistical significance. We will quote the lifetimes at the ℓ/σ_{ℓ} cuts listed in table I.

The background subtracted Monte Carlo corrected t' distributions for the four D^0 samples are shown in Fig. 6 along with the t' distributions of the side bands used to represent the background underneath the signal. The corresponding distributions for the D^+ are shown in Fig. 4b). Superimposed on each of the plots is a pure exponential function with the fitted lifetime value. In order to search for possible fit biases and to verify that the errors are estimated properly, several thousand Monte Carlo replicas of our final data samples were generated. These samples, identical in size to the final data samples, were generated using an exponential function to model the proper time evolution of the signal. The background proper time evolution was modeled by a sum of two exponential functions whose parameters were derived from the data. The distribution of the fitted lifetime from these simulated data samples revealed the presence of a small positive bias (overestimating the lifetime) of 0.001, 0.005, 0.002, and 0.002 ps, in the case of the $K^-\pi^+$ tag, $K^-\pi^+$ no-tag, $K^-\pi^+\pi^-\pi^+$ tag, and $K^-\pi^+\pi^-\pi^+$ no-tag samples respectively. All quoted lifetime values have been corrected for these biases. The statistical error calculated by the fitter was shown to be an underestimate of the true error due to neglected fluctuations in b_i . The corresponding statistical errors calculated by the fitter were subsequently increased (by 8%, 14%, 6%, and 10% respectively) to account for this effect. Table I shows the five measured lifetimes together with their statistical errors. The final value of the D^0 lifetime, obtained as the weighted average of the four measurements using statistical errors only, is 0.413 ± 0.004 ps. The confidence level of the hypothesis that the four D^0 lifetime measurements are consistent within statistical errors is 68%. The value of the D^+ lifetime is measured to be 1.048 ± 0.015 ps.

Systematic uncertainties in the lifetime measurements can arise from several sources. First, an error can be made due to uncertainties in the target absorption corrections. Two effects are present: hadronic absorption of secondaries which would increase the fitted lifetime if ignored; and absorption of the D in the target which would tend to decrease the fitted lifetime if not taken into account. The systematic error results from the uncertainty regarding the extent to which elastic scattering of charm secondaries can cause severe mis-measurement of the parent D and from the fact that the D absorption cross section is

unknown. We have simulated the total cross section of pions and kaons on beryllium with relative contributions of inelastic, elastic and quasi-elastic cross section from ref. [2], [4] and parameters of the elastic and quasi-elastic differential cross sections from ref. [5]. Uncertainties in this model caused negligible systematic errors in the lifetime. The D absorption cross section was modelled by the pion absorption cross section [4]. The systematic uncertainty due to this effect has been estimated by reducing the absorption cross section to half of the utilized value.

In general the acceptance of charm decay products depends on both the longitudinal and transverse position of the decay vertex due to the finite acceptance of the spectrometer. D mesons with higher momentum have higher acceptance on the average than those with lower momentum since they tend to decay closer to the microstrip system. The difference between the assumed D momentum distribution used for the calculation of the $f(t')$ correction factor and the true momentum distribution is a possible source of systematic bias. This systematic uncertainty has been estimated by fitting reduced proper time distributions of high and low momentum samples separately while utilizing the standard $f(t')$ correction factor.

The photon beam profile at the beryllium target determines the relative numbers of events occurring in the central and outer regions. The systematic error of the lifetime caused by the uncertainty in the photon beam profile has been estimated in a similar manner as the error associated with the D momentum distribution by fitting samples of inner and outer region events separately with the standard $f(t')$ correction factor.

Another source of systematic uncertainty comes from the uncertainty in the background time evolution caused by a choice of a particular combination of lower and upper sidebands to represent it. The magnitude of this uncertainty is estimated as the mean deviation of the lifetime obtained by using 25 – 75% and 75 – 25% mixtures of the low and high sidebands from the standard value obtained with a 50 – 50% mixture.

In addition, the finite statistics of the Monte Carlo samples leads to uncertainty in the calculated correction factor $f(t')$. In the case of our samples, this source introduces 0.003 ps systematic uncertainty in the lifetime measurements. Table II summarizes the estimates of

the systematic uncertainties discussed above for all the five samples.

In order to check our results for consistency and possible hidden biases each of the samples was fitted under different requirements and conditions including more stringent cuts and division (statistics permitting) of the data in various ways. No significant variation has been observed outside the statistical error bars for any of the five samples. Fig. 7 shows the result of these studies performed on the $K^-\pi^+\pi^+$ sample.

In order to obtain the final systematic error of the D^0 lifetime we have combined individual sources of systematic uncertainties for each of the four measurements with the assumption that the absorption and beam profile contributions are completely correlated between the four samples. To obtain the systematic uncertainty of the D^+ measurement we have combined individual contributions in quadrature. Combining all sources of systematic errors, we obtain the final lifetime values of $0.413 \pm 0.004(\text{statistical}) \pm 0.003(\text{systematic})$ ps for the D^0 and $1.048 \pm 0.015(\text{statistical}) \pm 0.011(\text{systematic})$ ps for the D^+ .

Using these two values and our previous result for the D_s lifetime [6] we obtain the following numbers for the ratios of charm meson lifetimes:

$$\frac{\tau(D^+)}{\tau(D^0)} = 2.54 \pm 0.04$$

and

$$\frac{\tau(D_s)}{\tau(D^0)} = 1.15 \pm 0.05$$

where the quoted errors are statistical.

In summary, new precise measurements of the D^0 and D^+ lifetimes based on samples of 16,000 and 9,000 fully reconstructed decays into $K^-\pi^+$, $K^-\pi^+\pi^-\pi^+$, and $K^-\pi^+\pi^+$ modes are reported. The lifetime of the D^0 is measured to be $0.413 \pm 0.004(\text{statistical}) \pm 0.003(\text{systematic})$ ps, while the D^+ lifetime is measured to be $1.048 \pm 0.015(\text{statistical}) \pm 0.011(\text{systematic})$ ps. Different data sets exhibited a high degree of consistency as observed through a very good agreement between the $K^-\pi^+$ and $K^-\pi^+\pi^-\pi^+$ samples and the tag and no-tag samples. We conclude by noting that our result will significantly decrease the errors on the current world average values [2] for the D^0 and D^+ lifetimes.

We wish to acknowledge the assistance of the staff of Fermi National Accelerator Laboratory, the INFN of Italy, and the staffs of the physics departments of the collaborating institutions. This research was supported in part by the National Science Foundation, the U.S. Department of Energy, the Italian Istituto Nazionale di Fisica Nucleare and Ministero dell'Università e della Ricerca Scientifica, and the Korean Science and Engineering Foundation.

REFERENCES

- ^a Present address: University of Maryland, College Park, MD, 20742, USA
- ^b Present address: Fermilab, Batavia, IL 60510, USA.
- ^c Present address: University of Colorado, Boulder, CO 80309, USA
- ^d Present address: Dip. di Fisica Nucleare e Teorica and INFN - Pavia, I-27100 Pavia, Italy
- ^e Present address: University of New York, Stony Brook, NY 11794, USA.
- ^f Present address: Yale University, New Haven, CN 06511, USA.
- [1] P.L. Frabetti *et al.*, Nucl. Instrum. Methods Phys. Res. **A 320**, (1992) 519.
- [2] Particle Data Group, K. Hikasa *et. al.*, Phys. Rev. **D 45**, (1992) 1.
- [3] P.L. Frabetti *et. al.*, Phys. Lett. **B 263**, (1991) 584.
- [4] S.P.Denisov *et. al.*, Nucl Phys. **B 61**, (1973) 62.
- [5] G.Bellettini *et. al.*, Nucl Phys. **B 79**, (1966) 609.
- [6] P.L. Frabetti *et. al.*, Phys. Rev. Lett. **71**, (1993) 827.

FIGURES

FIG. 1. Invariant mass distributions for the four D^0 samples: a) $K^-\pi^+$ tag sample for $\ell/\sigma_\ell > 5$; b) $K^-\pi^+$ no-tag sample for $\ell/\sigma_\ell > 13$; c) $K^-\pi^+\pi^-\pi^+$ tag sample for $\ell/\sigma_\ell > 6$; d) $K^-\pi^+\pi^-\pi^+$ no-tag sample for $\ell/\sigma_\ell > 10$.

FIG. 2. Invariant mass distributions for the $K^-\pi^+\pi^+$ sample for $\ell/\sigma_\ell > 15$.

FIG. 3. The correction factors $f(\Gamma)$ to the reduced proper time Γ as a function of Γ for the four D^0 samples: a) $K^-\pi^+$ tag sample for $\ell/\sigma_\ell > 5$; b) $K^-\pi^+$ no-tag sample for $\ell/\sigma_\ell > 13$; c) $K^-\pi^+\pi^-\pi^+$ tag sample for $\ell/\sigma_\ell > 6$; d) $K^-\pi^+\pi^-\pi^+$ no-tag sample for $\ell/\sigma_\ell > 10$.

FIG. 4. a) The fitted lifetime as a function of the ℓ/σ_ℓ detachment cut for the $K^-\pi^+\pi^+$ sample; The dot-dashed and dotted lines represent the previous world average lifetime value and its error respectively. b) The background subtracted and Monte Carlo corrected lifetime evolution of the $K^-\pi^+\pi^+$ sample for $\ell/\sigma_\ell > 15$ (shown as the solid-line histogram). The dashed-line histogram shows the side band Γ distribution used to represent the background. The straight line is an exponential with the fitted lifetime; c) The correction factor $f(\Gamma)$ to the reduced proper time Γ as a function of Γ for the $K^-\pi^+\pi^+$ sample.

FIG. 5. The fitted lifetime as a function of the ℓ/σ_ℓ detachment cut for the four D^0 samples: The dot-dashed and dotted lines represent the previous world average lifetime value and its error respectively.

FIG. 6. The background subtracted and Monte Carlo corrected lifetime evolution of the four D^0 samples (shown as the solid-line histograms): a) $K^-\pi^+$ tag sample for $\ell/\sigma_\ell > 5$; b) $K^-\pi^+$ no-tag sample for $\ell/\sigma_\ell > 13$; c) $K^-\pi^+\pi^-\pi^+$ tag sample for $\ell/\sigma_\ell > 6$; d) $K^-\pi^+\pi^-\pi^+$ no-tag sample for $\ell/\sigma_\ell > 10$. The dashed-line histogram shows the side band Γ distribution used to represent the background. The straight line is an exponential with the fitted lifetime.

FIG. 7. Plot of the D^+ lifetime obtained under different conditions: a) Anti-Particle lifetime; b) Particle lifetime; c) Tight Čerenkov requirements; d) Vertex isolation cuts; e) Upstream primary vertices; f) Downstream primary vertices; g) Upstream TR1 cut; h) Decays occurring in the vacuum; i) Explicit cut on the error of the primary and secondary vertex positions of 0.08 cm; j) Increased confidence level cut on the primary and secondary vertices; k) Low momentum D^+ events; l) High momentum D^+ events; m) Events near the target center; n) Events away from the target center; o) Background from low sideband only; p) Background from high sideband only; q) Fit to the proper decay times; r) Fit to the sample obtained by a stand alone vertexing algorithm. The dot-dashed line represents the standard fit value, while the dashed lines show the extent of the sum of systematic and statistical errors.

TABLES

TABLE I. Measured lifetimes

Sample	l/σ_l	Lifetime $\times 10^{-12}$ sec.
$K^-\pi^+$ tag	> 5	0.421 ± 0.009
$K^-\pi^+$ no-tag	> 13	0.405 ± 0.010
$K^-\pi^+\pi^-\pi^+$ tag	> 6	0.410 ± 0.010
$K^-\pi^+\pi^-\pi^+$ no-tag	> 10	0.413 ± 0.007
$K^-\pi^+\pi^+$	> 15	1.048 ± 0.015

TABLE II. Systematic uncertainties in 10^{-12} sec.

Sys.	$K\pi$ tag	$K\pi$ no-tag	$K3\pi$ tag	$K3\pi$ no-tag	$K\pi\pi$
Momentum	0.000	0.000	0.000	0.000	0.008
Absorp.	0.001	0.001	0.001	0.003	0.006
Beam prof.	0.001	0.001	0.001	0.001	0.001
Sidebands	0.002	0.006	0.002	0.002	0.003
$f(\Gamma^*)$	0.003	0.003	0.003	0.003	0.003
Total	0.004	0.007	0.004	0.005	0.011

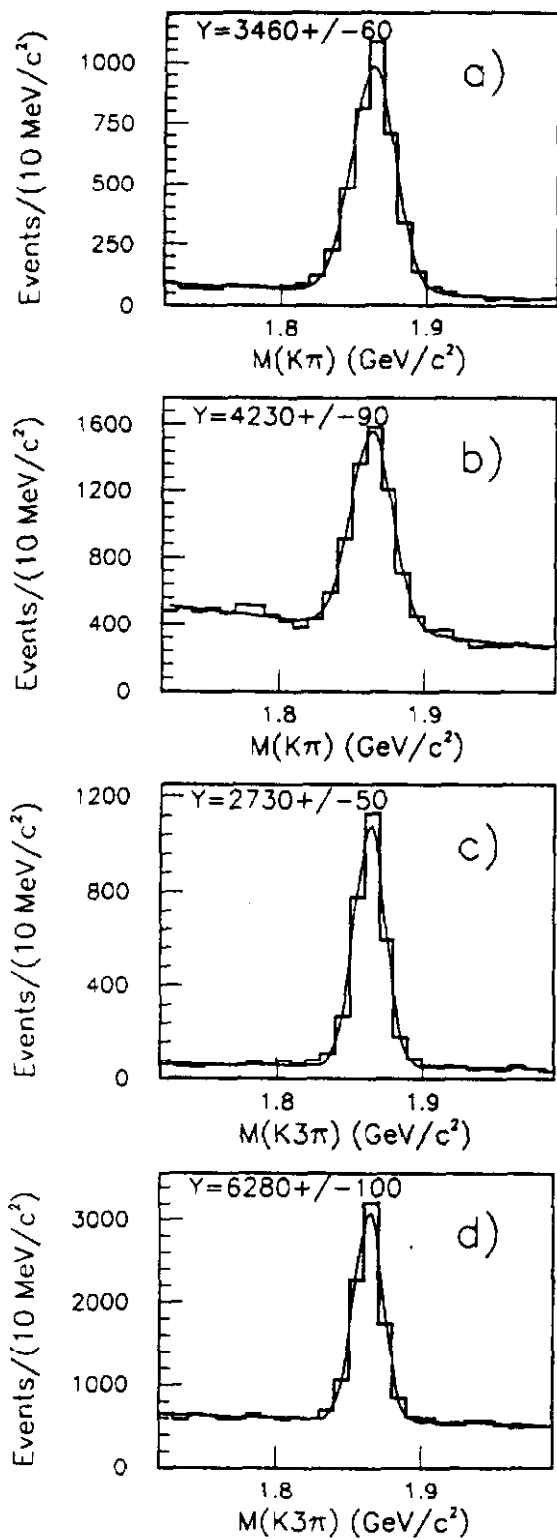


FIG. 1. Invariant mass distributions for the four D^0 samples: a) $K^-\pi^+$ tag sample for $\ell/\sigma_\ell > 5$; b) $K^-\pi^+$ no-tag sample for $\ell/\sigma_\ell > 13$; c) $K^-\pi^+\pi^-\pi^+$ tag sample for $\ell/\sigma_\ell > 6$; d) $K^-\pi^+\pi^-\pi^+$ no-tag sample for $\ell/\sigma_\ell > 10$.

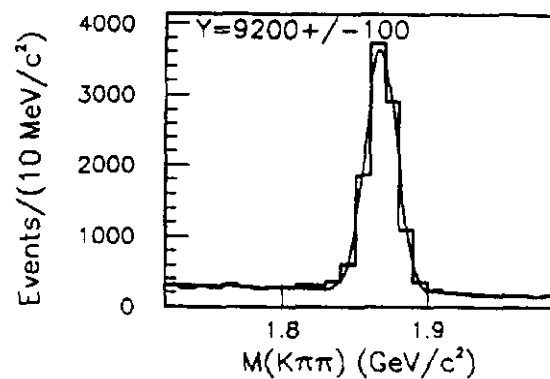


FIG. 2. Invariant mass distributions for the $K^-\pi^+\pi^+$ sample for $\ell/\sigma_\ell > 15$.

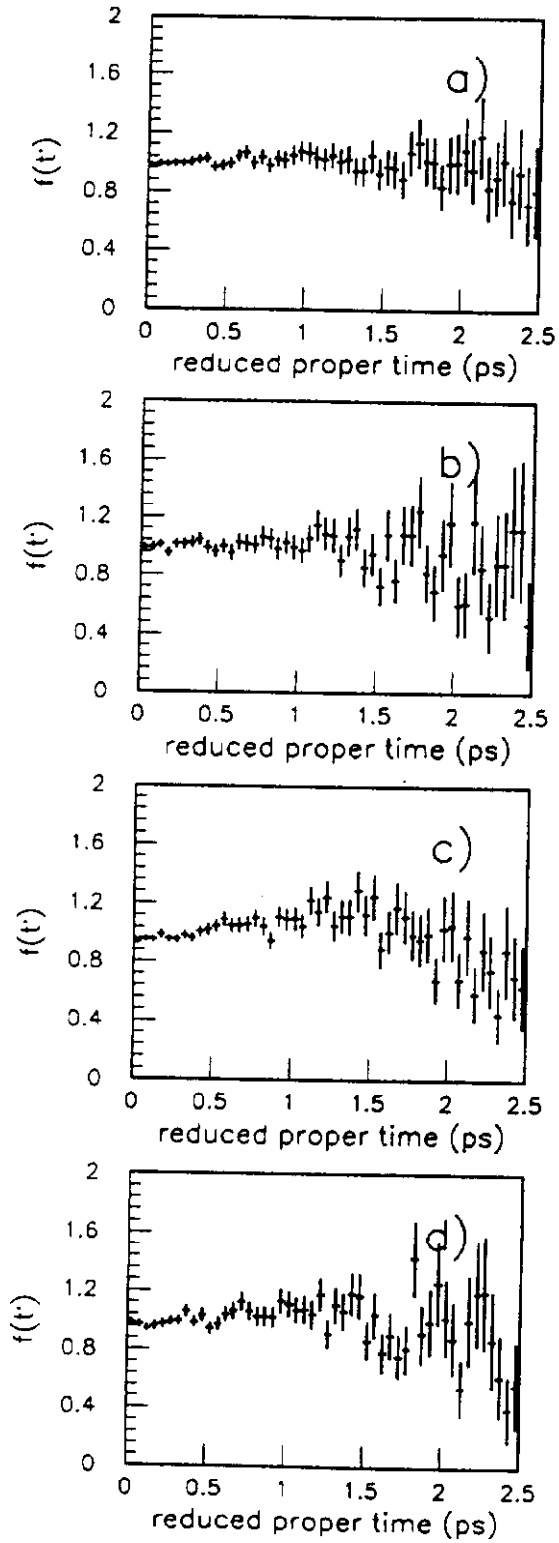


FIG. 3. The correction factors $f(t')$ to the reduced proper time t' as a function of t' for the four D^0 samples: a) $K^-\pi^+\pi^+$ tag sample for $l/\sigma_l > 5$; b) $K^-\pi^+$ no-tag sample for $l/\sigma_l > 13$; c) $K^-\pi^+\pi^-\pi^+$ tag sample for $l/\sigma_l > 6$; d) $K^-\pi^+\pi^-\pi^+$ no-tag sample for $l/\sigma_l > 10$.

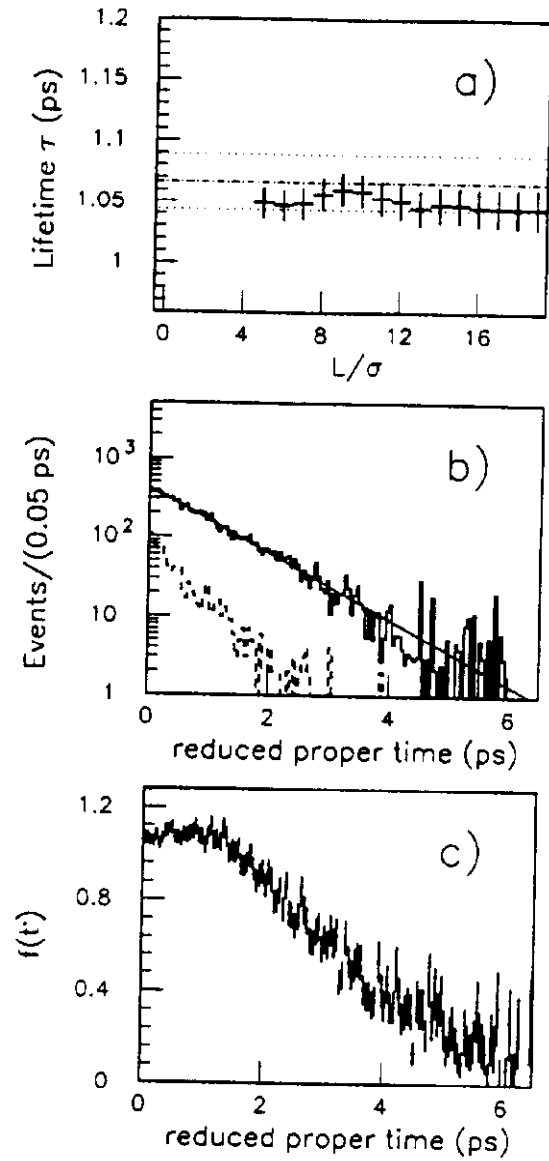


FIG. 4. a) The fitted lifetime as a function of the l/σ_l detachment cut for the $K^-\pi^+\pi^+$ sample; The dot-dashed and dotted lines represent the previous world average lifetime value and its error respectively. b) The background subtracted and Monte Carlo corrected lifetime evolution of the $K^-\pi^+\pi^+$ sample for $l/\sigma_l > 15$ (shown as the solid-line histogram). The dashed-line histogram shows the side band t' distribution used to represent the background. The straight line is an exponential with the fitted lifetime; c) The correction factor $f(t')$ to the reduced proper time t' as a function of t' for the $K^-\pi^+\pi^+$ sample.

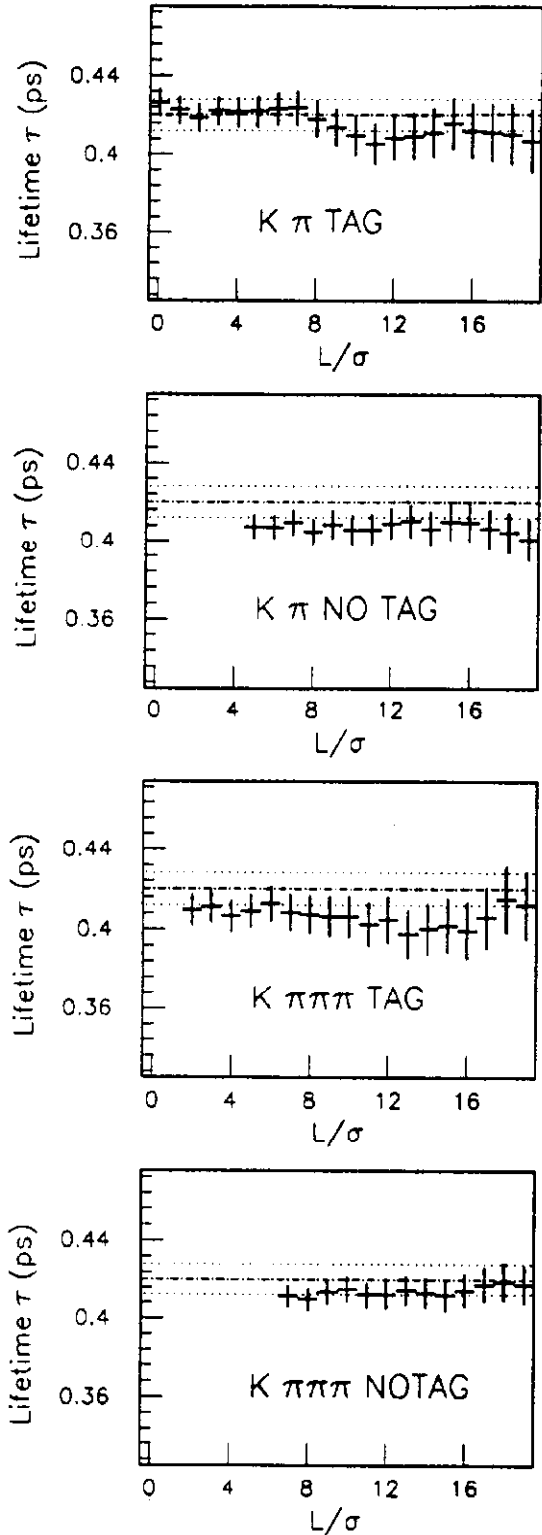


FIG. 5. The fitted lifetime as a function of the ℓ/σ_ℓ detachment cut for the four D^0 samples: The dot-dashed and dotted lines represent the previous world average lifetime value and its error respectively.

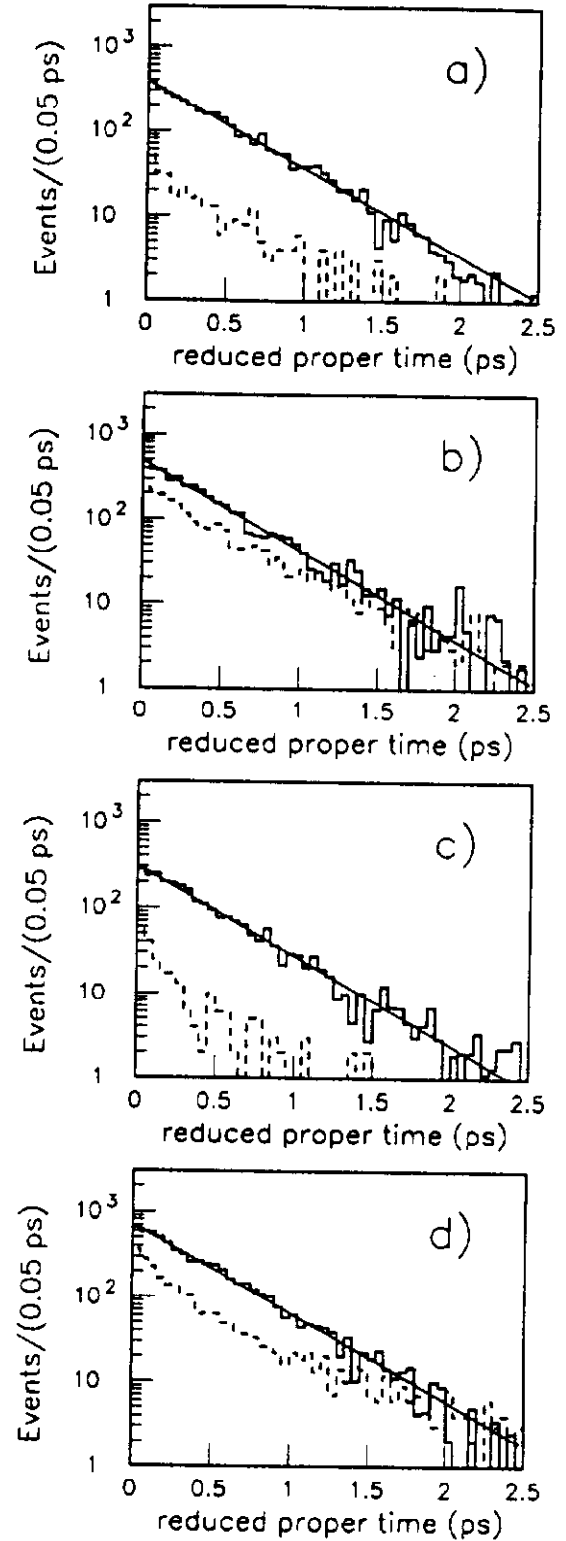


FIG. 6. The background subtracted and Monte Carlo corrected lifetime evolution of the four D^0 samples (shown as the solid-line histograms): a) $K^-\pi^+$ tag sample for $\ell/\sigma_\ell > 5$; b) $K^-\pi^+$ no-tag sample for $\ell/\sigma_\ell > 13$; c) $K^-\pi^+\pi^-\pi^+$ tag sample for $\ell/\sigma_\ell > 6$; d) $K^-\pi^+\pi^-\pi^+$ no-tag sample for $\ell/\sigma_\ell > 10$. The dashed-line histogram shows the side band t' distribution used to represent the background. The straight line is an exponential with the fitted lifetime.

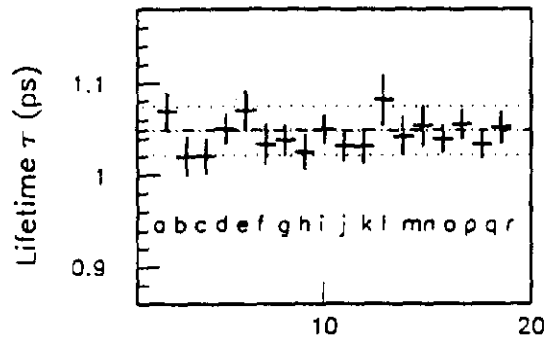


FIG. 7. Plot of the D^+ lifetime obtained under different conditions: a) Anti-Particle lifetime; b) Particle lifetime; c) Tight Čerenkov requirements; d) Vertex isolation cuts; e) Upstream primary vertices; f) Downstream primary vertices; g) Upstream TR1 cut; h) Decays occurring in the vacuum; i) Explicit cut on the error of the primary and secondary vertex positions of 0.08 cm; j) Increased confidence level cut on the primary and secondary vertices; k) Low momentum D^+ events; l) High momentum D^+ events; m) Events near the target center; n) Events away from the target center; o) Background from low sideband only; p) Background from high sideband only; q) Fit to the proper decay times; r) Fit to the sample obtained by a stand alone vertexing algorithm. The dot-dashed line represents the standard fit value, while the dashed lines show the extent of the sum of systematic and statistical errors.